Tuneable planar integrated optical systems

Tuneable planar integrated optical systems

M. Amberg[1], A. Oeder[1], S. Sinzinger[1], P. J. W. Hands[2], and G. D. Love[2]

[1] *TU Ilmenau, Dept. of Optical Engineering, P.O. Box 100565, 98684 Ilmenau, Germany*
[2] *Durham University, Dept. of Physics, South Road, Durham, DH1 3LE, UK*

martin.amberg@tu-ilmenau.de

Abstract: Planar integrated free–space optical systems are well suited for a variety of applications, such as optical interconnects and security devices. Here, we demonstrate dynamic functionality of such microoptical systems by the integration of adaptive liquid–crystal–devices.

OCIS codes: 200.4650; 050.1970; 130.0130; 010.1080

References and links

1. J. Jahns and A. Huang, "Planar integration of free space optical components," Appl. Opt. **28**, 1602-1605 (1994).
2. S. Sinzinger, "Microoptically integrated correlators for security applications," Opt. Commun. **290**, 69-74 (2002).
3. M. Gruber, J. Jahns, E. Joudi, and S. Sinzinger, "Practical Realization of Massively Parallel Fiber -Free-Space Optical Interconnects," Appl. Opt. **40**, 2902-2908 (2001).
4. A. F. Naumov, M. Y. Loktev, I. R. Guranik, G. V. Vdovin, "Liquid crystal adaptive lenses with modal control," Opt. Lett. **23**, 992-994 (1998).
5. A. F. Naumov, G. D. Love, M. Yu. Loktev, and F. L. Vladimirov, "Control optimisation of spherical modal liquid crystal lenses," Opt. Express **4**, 344-352 (1999).
6. P. J. W. Hands, A. K. Kirby, and G. D. Love, "Adaptive modally addresses liquid crystal lenses," Liq. Cryst. VIII, I.-C. Khoo ed., Proc. SPIE **5518**, 136-143 (2004).
7. G. D. Love, J. V. Major, and A. Purvis, "Liquid crystal prisms for tip-tilt adaptive optics," Opt. Lett. **19**, 1170-1172 (1994).
8. P. J. W. Hands, S. A. Tatarkova, A. K. Kirby, and G. D. Love, "Modal liquid crystal devices in optical tweezing: 3D control and oscillating potential wells," Opt. Express **14**, 4525-4537 (2006).
9. L. G. Commander, S. E. Day, and D. R. Selviah, "Variable focal length microlenses," Opt. Commun. **177**, 157-170 (2000).
10. G. D. Love, J. V. Major, and A. Purvis, "Liquid-crystal prisms for tip-tilt adaptive optics," Opt. Lett. **19**, 1170-1172 (1994).
11. M. Amberg, and S. Sinzinger, "Design considerations for efficient Planar Optical Systems," Opt. Commun. **267**, 74-78 (2006).
12. B. Wang, M. Ye, and S. Sasumo," Polarization–independent liquid crystal lens with four liquid crystal layers," IEEE Photonics Technology Lett. **18**, 79-81 (2006).
13. Q. Cao, M. Gruber, and J. Jahns, "Generalized confocal imaging systems for free-space optical interconnections," Appl. Opt. **43**, 3306-3309 (2004).
14. M. Testorf and J. Jahns, "Imaging properties of planar-integrated micro-optics," J. Opt. Soc. Am. A **16**, 1175-1183 (1999).
15. S. Masuda, S. Takahashi, T. Nose, S. Sato, and H. Ito, "Liquid-crystal microlens with a beam-steering function," Appl. Opt. **36**, 4772-4778 (1997).
16. S. Sinzinger and J. Jahns, "Integrated microoptical imaging system with high interconnection capacity fabricated in planar optics," Appl. Opt. **36**, 4729-4735 (1997).
17. J. Jahns, V. Arrizn, D. Hagedorn, S. Kinne, and S. Sinzinger, "Sensing applications of planar integrated free-space optics with broadband illumination", poster presentation at " Conference on Light-Emitting Diodes: Research, Manufacturing, and Applications II", "SPIE International Symposium on Optoelectronics," San Jose, CA, USA (1998).

#82257 - $15.00 USD Received 19 Apr 2007; revised 25 May 2007; accepted 25 May 2007; published 7 Aug 2007

1. Introduction

Planar integrated free space optics [1] (PIFSO) combines the advantages of free space optics with the precise alignment possibilities of planar fabrication technology. Due to their robustness these systems are well suited e.g. for optical interconnects, relay systems and security applications [2, 3]. A variety of planar systems has been demonstrated so far which exclusively show static optical functionality. In this letter we present a planar integrated $4f$–imaging system combined with a modal liquid crystal (LC) lens [4, 5] and a LC–prism to demonstrate adaptive PIFSO. These set–ups can be used for scanning, beam splitting, for active alignment of systems that suffer from substrate thickness tolerances and prospective for integrated optical tweezing systems for 3–D control as shown for non integrated systems in [8].

There are a variety of techniques [9] for producing variable LC–lenses. Modal devices [5, 4] were chosen because of their simplicity, the continuity of the phase profile (and thus high efficiency), and the fact that the focal length can be continuously changed. Furthermore it is possible to produce tip/tilt phase profiles [10] with the same structures which means that the transverse position of the image can also be shifted. However it would be also possible to use other adaptive LC–structures.

In section 2 we introduce the concept of planar integrated free–space optical systems and in section 3 we explain the structure and functionality of analog liquid crystal (LC) lenses. Section 4 focuses on the design considerations and functional estimates for the combination of PIFSO system with LC–lenses followed by the presentation of a first demonstrator system in section 5 and its results for focus shifts and beam deflection in section 6 and section 7. Section 8 concludes the paper.

2. Introduction to planar integrated free-space optics

The concept of PIFSO is to fold the optical system into a thick glass substrate (see Fig. 1). Optical elements, either diffractive or refractive ones, can be integrated on the surfaces of the substrate. Thus the light travels between the reflection–coated surfaces of the substrate on a zigzag path. In the case of purely diffractive systems the employment of micro technological methods allows precise alignment of the optical components during the mask layout process. The fabrication of these systems is possible with standard lithographic and etching technology. After fabrication these systems are ready to run without further alignment steps. The integration of refractive elements is possible with the help of lithographical alignment features. In the future, fully integrated planar optical systems employing diffractive and refractive optical elements could be fabricated by ultra precision micromachining.

3. Analog liquid crystal (LC) elements

The combination of (modal) LC–optical elements enables the implementation of dynamic optical microsystems. For our demonstration system we aim to produce a continuous variation of the focal spot using a modal LC–lens [4, 5, 6]. Conventional zonal addressing uses pixelated electrode structures, which generate discrete step-wise changes to the phase profile across the aperture of the device. Conversely, modal addressing generates a continuously varying phase profile across the device's aperture, the shape of which can be adjusted according to the shape of the electrodes, the driving voltage and the frequency.

The modal LC–lens used in this paper (Fig. 1(a) consists of a 20μm layer of LC (kept in anti-parallel alignment by adjacent rubbed polyimide layers) sandwiched between two electrode substrates. Electrode one (connected to 0V) is made from silver and is both conductive and reflective. The second electrode (connected to a high frequency AC voltage) is transparent and has a much higher electrical resistance. This electrode is made from Baytron conductive polymers

#82257 - $15.00 USD Received 19 Apr 2007; revised 25 May 2007; accepted 25 May 2007; published 7 Aug 2007

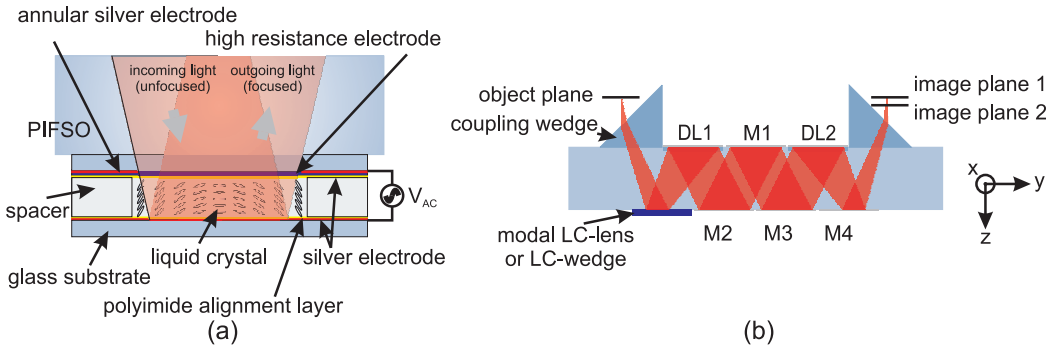

Fig. 1. a) Set–up of the modal LC–lens added to the PIFSO and b) Set–up of the prism–coupled adaptive PIFSO experiment; DL 1 and DL 2 mirror coated diff. lenses and M1-M4 plane mirrors

and is surrounded by an annular silver electrode aperture. A non-linear and quasi-parabolic voltage (and therefore also phase) profile can be distributed across the device through control of the electrical supply voltage and frequency, resulting in electrically adaptive control of lens aberrations and focal length. Additional control over the power of the lens can also be provided by careful modification of the sheet resistance of the high resistance electrode.

Beam-steering devices based upon similar modal LC–elements can also be implemented by instead applying a voltage to dual parallel electrodes located on the high resistance substrate [7, 8]. In this situation, the LC–layer then acts as an adaptive optical prism.

In order to demonstrate significant adaptive optical functionality in integrated optical systems it is necessary to achieve sufficient maximum optical power of the integrated modal LC lenses. The designs show that numerical apertures of about 0.01 need to be achieved. This is beyond what has been achieved for macroscopic modal LC lenses. Stronger lens profiles (for a given LC–material) can either be realised by increasing the thickness of the LC–layer (at the expense of increasing the response time) or by reducing the aperture of the modal lens. Since the power depends on the inverse square of the lens diameter we concentrated on producing small lenses with diameters of around $d_{\text{aperture}} = 3\text{mm}$. The key parameter for the fabrication in this case is the correct sheet resistance of the high resistance electrode. In order to get the maximum phase profile for different lens diameters while retaining reasonable driving parameters (10kHz, 5-10V), the high resistance electrode has to be adjusted according to the aperture size.

The right values for this correction result from a thorough parameter study for lenses with apertures between $d_{\text{aperture}} = 3 - 7\text{mm}$ (Fig. 2). For lenses 3mm in diameter a maximum phase shift can be achieved with a resistance of 10^8Ohm. As an electrode material we found Baytron AI 4083 to meet this specification. Typical values for the maximum phase shift of a transmissive modal LC–lens with a $20\mu\text{m}$ thick LC–layer are about $10\times 2\pi$. For an element used in reflection the phase shift doubles as the light travels two times through the birefringant LC–material. Thicker LC–layers also lead to higher phase shift.

4. Design considerations for a combined planar integrated free-space optical system with an adaptive modal lens

In order to demonstrate the potential of an adaptive PIFSO we combined a purely diffrative planar integrated $4f$–imaging system with a modal LC–lens and a modal LC–prism. The optical system design is based on a generalized confocal imaging system for free–space optical

#82257 - $15.00 USD Received 19 Apr 2007; revised 25 May 2007; accepted 25 May 2007; published 7 Aug 2007

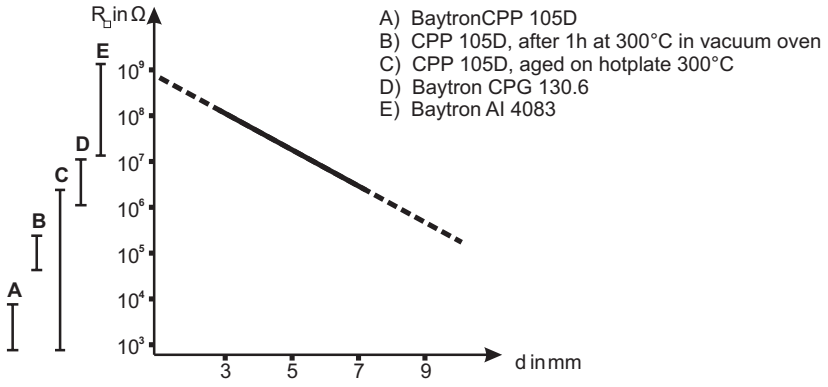

Fig. 2. Target resistances of the high resistance layer and values for different electrode material: A) Baytron CPP 105D B) CPP 105D, after 1h at 300°C in vacuum oven C) CPP 105D, aged on hotplate 300°C D) Baytron CPG 130.6 E) Baytron AI 4083

interconnects suggested by Cao et. al. [13]. The conventional $4f$–set–up can be adapted for different distances d_1 and d_2 by adding a field lens F (see Fig. 3) with negative power. In our design considerations we vary the distance d_2 of 2.4mm in a planar optical system through an integrated LC–lens acting as the field lens F. For this shift the necessary phase shift is $40 \times 2\pi$ for a LC–lens of 5mm in diameter.

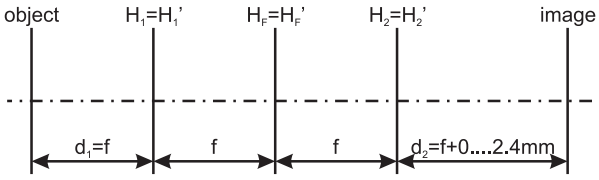

Fig. 3. Schematic representation of an unfolded generalized confocal imaging system according to Ref. [8]

The ZEMAX™ simulations shown in Fig. 4 illustrate the theoretical potential of this integrated adaptive microsystem. We modeled the set–up with $d_1 = f$ and $d_2 = f + 0 \ldots 2.4$mm. The spot diagrams in Fig. 4 show an object field of 2 x 2mm^2 with the object points located at

$$(x,y) = \begin{pmatrix} 1,1 & 1,0 & 1,-1 \\ 0,1 & 0,0 & 0,-1 \\ -1,1 & -1,0 & -1,-1 \end{pmatrix} \tag{1}$$

for $d_2 = f$ and $d_2 = f + 2.4$mm.

These simulations show the good optical properties of this configuration. The rms spot sizes remain smaller than $r = 0.4\mu$m for the whole image field. For $d_2 = f$ the field is ideally imaged with a magnification of $\beta' = -1$ but when moving the image plane apart from the substrate surface ($d_2 = f + 2$mm) the image is slightly trapezoidal distorted . Thus the object point $(x,y) = (-1\text{mm}, -1\text{mm})$ is imaged to $(x',y') = (0.998\text{mm}, 0.998\text{mm})$ and $(x,y) = (1\text{mm}, 1\text{mm})$ to $(x',y') = (-1.001\text{mm}, 1.002\text{mm})$ while the spot for $(x,y) = (0\text{mm}, 0\text{mm})$ re-

#82257 - $15.00 USD Received 19 Apr 2007; revised 25 May 2007; accepted 25 May 2007; published 7 Aug 2007

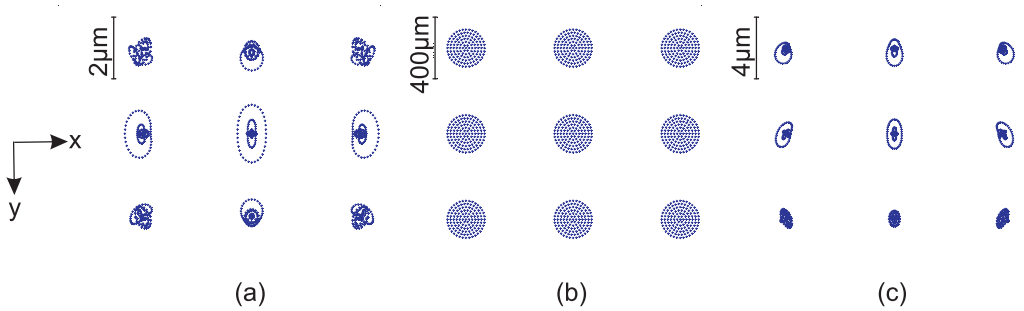

Fig. 4. Spotdiagrams for a) $d_2 = f$ and LC–lens switched off, b) for $d_2 = f + 2.4$mm and LC–lens switched off and c) $d_2 = f + 2.4$mm and LC–lens switched on with a maximum phase shift of $40 \times 2\pi$.

mains at $(x', y') = (0\text{mm}, 0\text{mm})$. These ray–tracing simulations obviously neglect diffraction effects. Since the optical system is folded into a glass substrate the light hits the diffractive lenses at an oblique angle. Thus the focal length in the two coordinate axes x and y is calculated in order to avoid astigmatism [14]. Oblique incidence also occurs at the LC–lens. Thus we calculated the required astigmatic ratio of the focal lengths over the full tuning range to see if there was any serious variation. The results shown in Fig. 5 show a deviation of the astigmatic ratio of $5.5 \times 10^{-}5$ for the tuning range, which is negligible. Figure 5 also shows the maximum necessary phase shift (in 2π) for the integrated LC–lens.

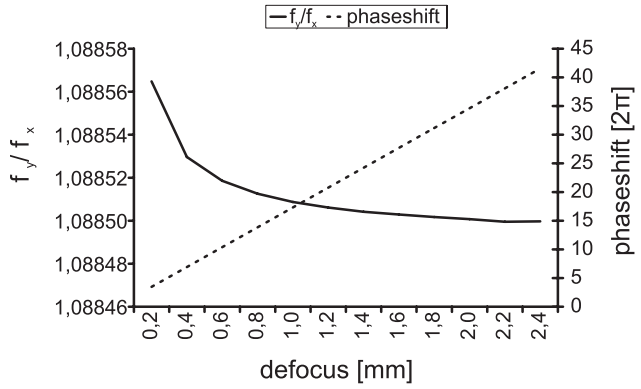

Fig. 5. Ratio of the focal length in x– and y–direction (bold line) of the LC–lens and the needed phase shift in $\times 2\pi$ for a defocus of 0mm...2.4mm (dotted line)

Instead of a focus shift by a field lens it is possible to use a prism for beam deflection. Thus it is possible to scan in the x–y–direction in the image plane of the system. The maximum deflection is a function of the prisms width and the birefrigance of the material. For a phase shift of $20 \times 2\pi$ the maximum deflection is about 35μm in x– and y–direction. Due to the low deflection angle it is necessary to implement the LC–prism as far as possible away from the image plane as we did in the experimental set–up (see sec. 7). It is also possible to combine tip/tilt and lensing function within a single LC–element as proposed in [15].

#82257 - $15.00 USD Received 19 Apr 2007; revised 25 May 2007; accepted 25 May 2007; published 7 Aug 2007

5. Experimental set–up of a tunable planar integrated free-space optical system

For our experiment we started with a prism coupled system as suggested in [11] (Fig. 1(b). The system is composed of 4 glass wafers, a 1mm thick fused silica substrate with the etched diffractive lenses DL1 and DL2 and the alignment marks for the coupling prisms, two unstructured 5mm fused silica substrates as spacers and an additional 1mm fused silica substrate on the bottom with the plane mirror coating (M2-M4). For adding the LC–lens, we removed the substrate on the bottom of the system to replace it by the LC–lens which is also fabricated on a 1mm glass substrate. For the experiment we used positive LC–lenses. Thus by addressing the LC–lens the focus of the system can be shifted towards the substrate surface from image plane 1 to image plane 2 (Fig. 1(b). For practical reasons the position of the modal lens in the system is located at the first reflection on the bottom of the system.

The experiments were performed at a wavelength $\lambda = 632.8$nm. The beam of a 5mW He–Ne laser is coupled to a single mode fibre. This fibre tip serves as a point source which could be aligned in the object plane. The laser light is coupled into the glass substrate by a refractive prism at a coupling angle of $\alpha = 11.77^{\circ}$. After the laser light is coupled out of the system by another refractive prism, the spot is imaged by a microscope objective onto a CCD chip.

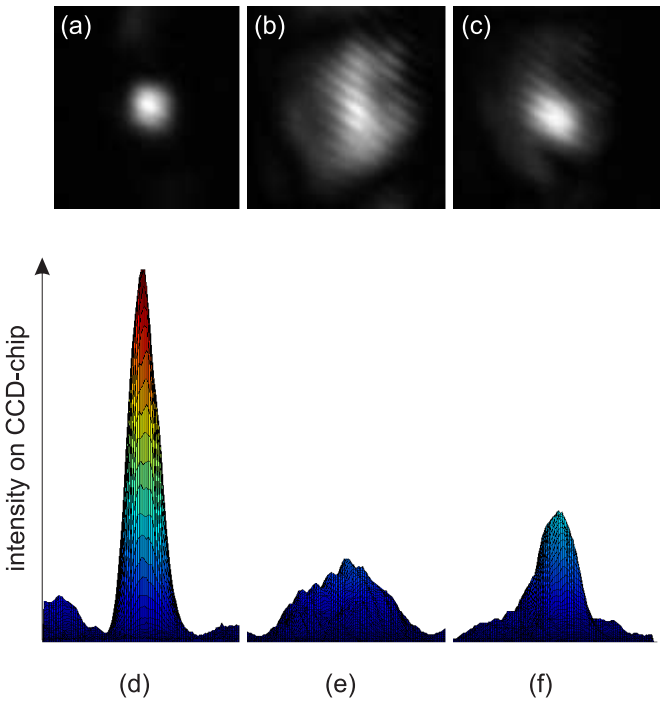

Fig. 6. Spots from the experimental set–up for focus plane tuning. a) spot captured by a CCD camera at image plane 1, b) captured spot for the system defocused to image plane 2 and c) captured spot corrected with the LC–lens at image plane 2. Figures d,e and f show the intensity plots generated with Matlab™ from the data of the CCD camera for the spots in a), b), and c) respectively.

#82257 - $15.00 USD Received 19 Apr 2007; revised 25 May 2007; accepted 25 May 2007; published 7 Aug 2007

6. Results for the focus shift by a modal LC–lens

Figures 6(a)–(f) show the results of the images of a point source $((x,y) = (0,0))$ in the image planes 1 and 2 with an active and inactive modal LC–lens. Fig. 6(a,b,c) and (d,e,f) show the spot captured by the CCD camera with a window sized 38.8 x 38.8 μm^2 and the intensity plots of the spots generated from the CCD camera data with Matlab™ respectively. Figure 6(a) and (d) is the captured spot at image plane 1 (compare Fig. 1) with an active LC–lens. The camera is set to an exposure time ET = 13.38ms to get a non saturated spot picture. In Fig. 6(b) and (e) the optical system is defocused by 300μm to image plane 2. The exposure time for Fig. 6b is set again to get full dynamic range picture (ET = 58ms) and Fig. 6(e) for better comparison again to ET = 13.38ms. For imaging correction the LC–lens was turned on to focus the spot in image plane 2. This is leading to a spot as seen in Fig. 6(c) for a full dynamic range image (ET = 37.5ms) and Fig. 6(f) again with ET = 13.38ms for comparison with the other two spots. All spots were captured with a polarising filter in front of the CCD–camera. The spot focused on image plane 1 and the corrected spot on image plane 2 show good optical properties with Gaussian shape. The size for the spots ($1/e^2$) in Fig. 6(d) and 6(f) is 9.5μm and 20μm respectively. The efficiency (Strehl ratio) for the corrected spot (active LC–lens) is about $\eta = 0.35$ compared to the focussed spot with an inactive LC–lens. This relatively low value is caused by aberrations in the lens, but these could be ameliorated by more complex drive voltages, as described in Ref. [5]. The integration of the intensity across an fixed size area around each of the two spots shows that 80% of the initial intensity of the spot on image plane 1 is in the area around the corrected spot on image plane 2.

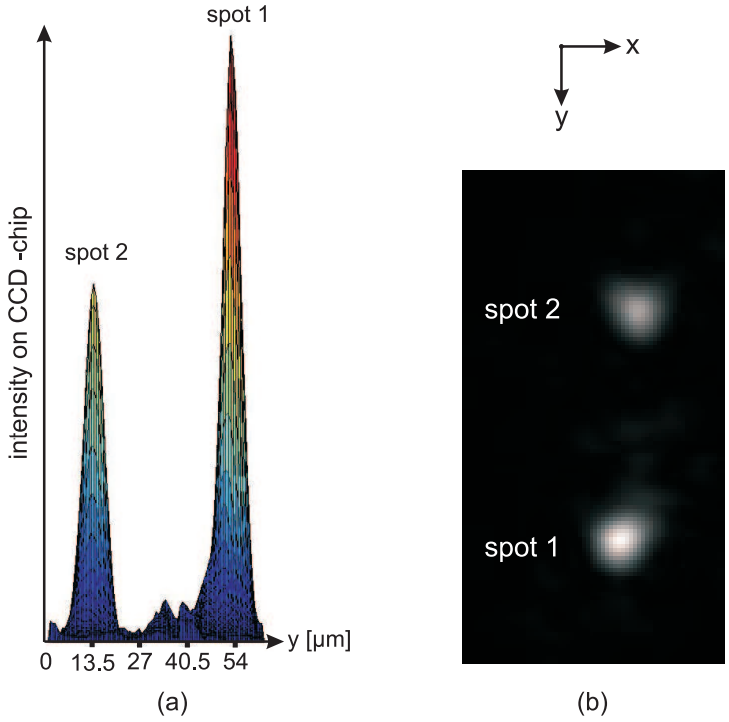

Fig. 7. Spots from the experimental set–up for beam deflection. a) intesity plot of the non deflected spot1 and of the deflected spot 2 b) spots captured taken by a CCD camera (spots are copied to a single picture).

#82257 - $15.00 USD Received 19 Apr 2007; revised 25 May 2007; accepted 25 May 2007; published 7 Aug 2007

7. Results for deflection by a modal LC–prism

Compared to the experiment in sec. 6 we exchanged the modal LC–lens with a modal LC–prism (width 2.5mm) for beam deflection. Thus it is possible to shift the focus in the x–direction by about $a_{\text{deflect}} = 39\mu$m. Within our set–up the needed phase shift for such a deflection of about $16 \times 2\pi$ across the LC–prism. Figs. 7(a) and (b) show the results for the beam deflection where the two spots are copied to a single picture and the exposure time is constant (exposure time ET = 44ms). Figure 7(a) is the picture captured by a CCD, and 7(b) is a cross section of the spot in 7a generated with Matlab™. For the deflected beam there is a high intensity loss of about 40%. The loss is caused by scattering effects in the LC–prism. The integration of the intensity across an fixed size area around each of the two spots shows that nearly 99% of the initial intensity of spot 1 is brought in the area around spot 2. The results are generated with a polarisation filter in front of the camera. When running the experiment without a polarising filter, beam splitting abilities of the LC–elements can be demonstrated as just the polarisation direction parallel to the rubbing direction of the alignment layer is sensitive to phase modulations by the liquid crystal. So just half of unpolarized light will be deflected by the prism while the other part is imaged undeflected to the CCD. The spot size ($1/e^2$) is about 12.3μm in diameter with good optical quality for both switching conditions.

8. Conclusion

In this paper we demonstrated the combination of a planar integrated free–space optical system and modal LC–devices for focus tuning and beam deflection. A focus shift in z–direction of the image plane of 300μm and a beam deflection of about 40μm was demonstrated with good optical quality. Design considerations for integrated adaptive microsystems have been performed. These dynamic tuning ranges will be very useful for an adaptive optimization of the integrated planar optical systems which become necessary in case of temperature or wavelength drifts. For densely packed optical interconnect applications lateral channel distances of the order of several 10's of microns are discussed [16]. Thus, the system introduced here will allow for the dynamic switching between different output channels dynamically. Further applications will be found in integrated optical sensing systems, i.e. integrated confocal sensors [17].

Acknowledgments

This work, as part of the European Science Foundation EUROCORES Program SPANAS, was supported by funds from the Deutsche Forschungsgemeinschaft DFG and the EC Sixth Framework Program. Further funding is supported by the Thueringer Wirtschaftsministerium within the project "Mikrooptische Pinzette."

#82257 - $15.00 USD Received 19 Apr 2007; revised 25 May 2007; accepted 25 May 2007; published 7 Aug 2007